Conjugation of substituted naphthalimides to polyamines as cytotoxic agents targeting the Akt/mTOR signal pathway

Zhi-yong Tian,[a,b] Song-qiang Xie,[c] Zi-hou Mei,[d] Jin Zhao,[a] Wen-yuan Gao*[b] and Chao-jie Wang*[a]

Received 29th June 2009, Accepted 3rd August 2009
First published as an Advance Article on the web 3rd September 2009
DOI: 10.1039/b912685f

Though several naphthalimide derivatives have exhibited antitumor activity in clinical trials, some issues such as toxicity prompted further structural modifications on the naphthalimide backbone. A series of naphthalimides conjugated with polyamines were synthesized to harness the polyamine transporter (PAT) for drug delivery, which was beneficial for the tumor cell selectivity. Bioevaluation in human hepatoma HepG2 cells treated with α-difluoromethylornithine (DFMO) or spermidine (Spd), human hepatoma Bel-7402 and normal QSG-7701 hepatocyte confirmed the PAT recognition and cell selectivity. In addition, the novel naphthalimide polyamine conjugate kills cells *via* apoptosis, and the Akt/mTOR signal pathway was first identified as the upstream cellular target through the apoptotic mechanism research. The presence of DFMO or Spd only either elevated or attenuated the cell apoptosis, but did not change the signal pathway. Collectively, the proper polyamine recognition element (*i.e.*, homospermidine) mediated effective drug delivery *via* the PAT, and helped the proper cytotoxic goods (*i.e.*, diverse naphthalimides) exert antitumor properties.

Introduction

As a common chemical motif, naphthalimides are among a growing class of compounds with desirable anticancer activity. Numerous mono- or bis-naphthalimide derivatives displayed potent antitumor properties against a variety of murine and human tumor cells, and some of them have been tested in the clinic for the treatment of solid tumors.[1] However, most clinical trials have failed because of a poor therapeutic index, or dose-limiting bone marrow toxicity. Subsequent efforts to improve therapeutic properties of naphthalimides have been made by modifying the naphthalimide skeleton.[2] Further novel analogues continue to be evaluated in experimental cancer models.[3]

Targeted antineoplastic therapies continue to be of interest because the more selective drugs harm fewer normal cells, and thus reduce side effects. One rational strategy to improve the drug selectivity is to incorporate the drug with a special vector which can recognize the tumor cells. Previous studies reveal that polyamines are such a promising carrier which transports cytotoxic agents into cancer cells.[4] Polyamines are important for tumor cell growth and function. The biosynthetic pathway of native polyamines (putrecine, spermidine and spermine) has been a popular target for the therapeutic intervention during the last decades.[5] Tumor cell types can import native polyamines from exogenous sources *via* the active polyamine transporter (PAT) to sustain their growth, especially if the biosynthesis pathway is blocked. Because the PAT can tolerate some structurally modified polyamines,[6] drug-polyamine conjugates as a special polyamine derivative can mimic the native ones and enter cells by PAT.

Systematic investigations have helped to define some key structure-activity relationships of drug-polyamine conjugates.[7] Future work should be focused both on searching for cytotoxic cargoes matched with known polyamine vectors, and on identifying the corresponding cellular targets. As a planar tricyclic DNA intercalator greatly similar to anthracene, the naphthalimide was supposed to be one ideal candidate according to the earlier lead compound anthracenylmethyl-homospermidine (Fig. 1, compound **1**).[4] Indeed, our work proved that such conjugates (Fig. 1, compounds **2**, **3**), composed of a 1,8-naphthalimide unit covalently attached to a polyamine such as spermidine or homospermidine, possessed remarkable cell selectivity through human hepatoma Bel-7402 and human normal hepatocyte QSG-7701 trials.[8] In addition, one representative conjugate, N^4-(naphthalimide-butyl)-homospermidine (**3**), killed tumor cells *via* apoptosis.[8] These results encouraged us to test more substituted naphthalimide polyamine conjugates in order to assess their PAT recognition,

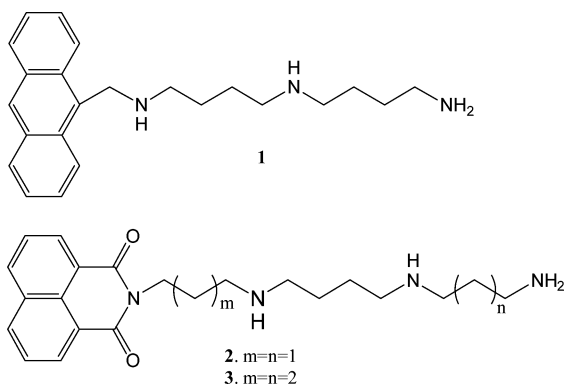

Fig. 1 The structures of compound **1**, **2** and **3**.

[a]*Key Laboratory of Natural Medicine and Immuno-Engineering, Henan University, Kaifeng, 475001, China. E-mail: wcjsxq@henu.edu.cn; Fax: +86-378-2864665*
[b]*School of Pharmaceutical Science and Technology, Tianjin University, Tianjin, 300072, China. E-mail: pharmgao@tju.edu.cn; Fax: +86-22-87401895; Tel: +86-22-87401895*
[c]*College of Pharmacy, Henan University, Kaifeng, 475001, China*
[d]*Chemistry Department, Henan University, Kaifeng, 475001, China*

cell selectivity, and more importantly, to elucidate the upstream cellular target.

Results

Synthesis of substituted naphthalimide polyamine conjugates

The polyamine conjugates with four different substituents on the naphthalimide backbone were prepared from triprotected tetraamine motifs and related 1,8-naphthalic anhydrides. Three starting anhydrides, including 4-chloro-1,8-naphthalic anhydride (**4**), 4-bromo-1,8-naphthalic anhydride (**5**), and 3-nitro-1,8-naphthalic anhydride (**6**), were commercially available. 3-amino-1,8-naphthalic anhydride was prepared from **6** by reduction of the nitro group.[9] The Boc protection of the resulted amino group by routine approaches[4] furnished the related anhydride (**7**) which was suitable for the next reaction.

The synthetic route toward the target conjugates **10a**-**10i** is shown in Scheme 1. The tri-Boc protected tetraamines **8a**, **8b** and **8c** were prepared according to a modified procedure reported previously.[10] The condensation of **8** with different anhydrides in absolute ethanol at reflux for 3 hours generated intermediates **9**. Subsequently the Boc groups of pure **9** were removed with 4M HCl at room temperature to afford target compounds **10** as hydrochloride salts in 60-80% yield.[4] The structures of the target compounds were confirmed by ^{1}H NMR, ^{13}C NMR, ESI-MS, and elemental analysis.

PAT recognition and cell selectivity

The *in vitro* cytotoxicities of novel conjugates were assessed by the MTT assay in the presence of aminoguanidine (an inhibitor of amine oxidase) against five cell lines, human leukemia K562, breast cancer MDA-MB-231, prostate cancer LNCaP, Bel-7402 and HepG2. As shown in Table 1-3, most conjugates displayed potency to K562, MDA-MB-231, Bel-7402 and HepG2 cells. In addition, some conjugates possessed equivalent potency to lead compound **3**. All the naphthalimide polyamine conjugates are not sensitive to LNCaP cells while anthracene polyamine conjugate **1** was toxic to all tested cells.

A previous report revealed that the presence of polyamines in conjugate **3** resulted in selectivity to cancer cells through Bel-7402 and normal QSG-7701 trials.[8] Therefore experiments are undertaken to examine the effect of several conjugates on QSG-7701 cell proliferation. The IC_{50} values of **10a**, **10f** and **10h** in Table 2 proved that they were much less toxic to the human normal hepatocyte as compared to the hepatoma cells in spite

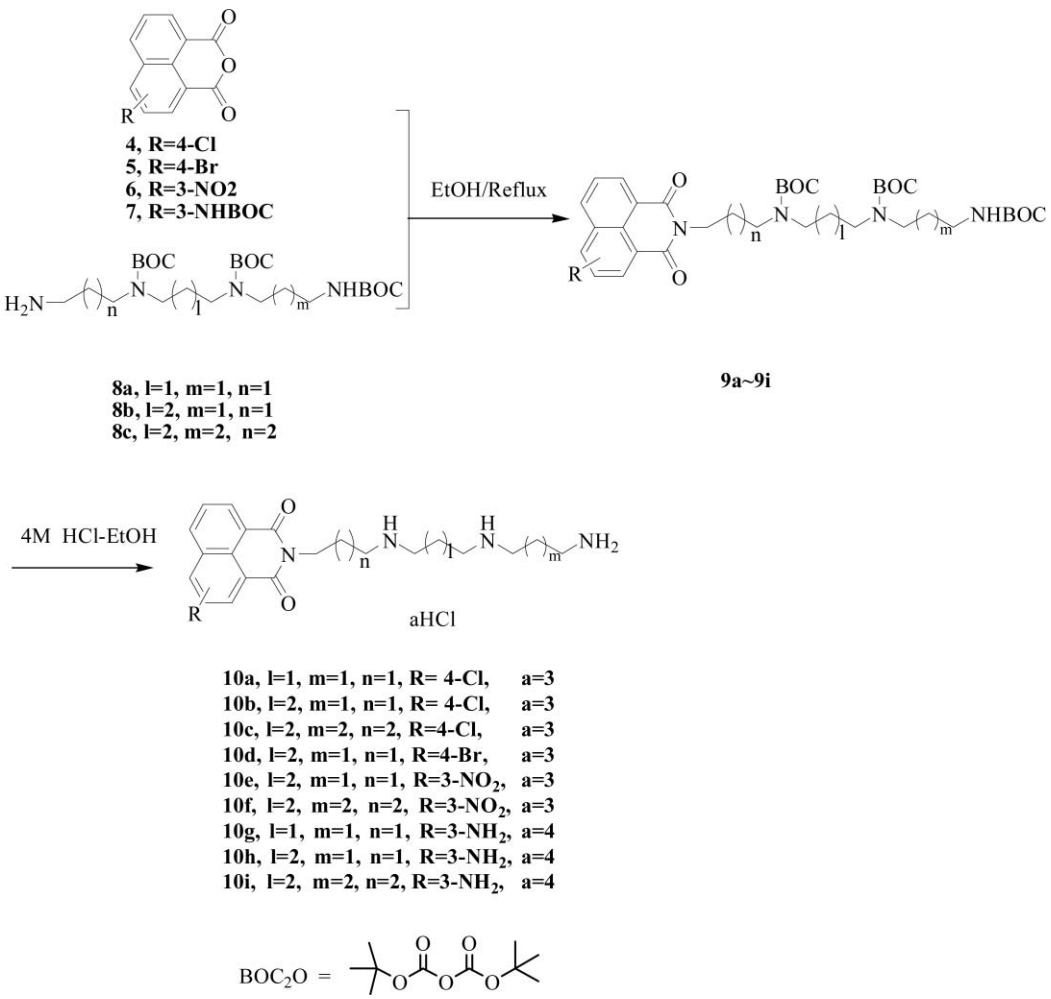

Scheme 1 Synthesis of naphthalimide polyamine conjugates.

Table 1 *In vitro* activity of polyamine conjugates on K562, MDA-MB231 and LnCap cells

	IC_{50}(μM)		
Compd	K562	MDA-MB-231	LnCap
10a	10.18 ± 0.13	1.25 ± 0.13	20.38 ± 0.82
10b	9.41 ± 0.23	7.83 ± 0.15	>50
10c	1.23 ± 0.05	5.75 ± 0.66	>50
10d	2.66 ± 0.16	6.8 ± 0.66	>50
10e	12.38 ± 1.73	—	—
10f	5.10 ± 0.68	44.1 ± 2.94	>50
10g	3.01 ± 0.11	6.13 ± 0.26	>50
10h	52.7 ± 3.67	6.33 ± 0.98	>50
10i	1.73 ± 0.12	8.95 ± 1.35	>50
3	1.16 ± 0.05	—	—
1	0.85 ± 0.04	0.53 ± 0.05	3.57 ± 0.24
Amonafide	>50	16.18 ± 0.61	>50

All data are expressed as means ± SD from three separate determinations. IC_{50} values were given only if they were less than 50 μM, which was the maximum concentration tested.

Table 2 *In vitro* selectivity of polyamine conjugates on BEL-7402 and QSG-7701 cells

	IC_{50} (μM)	
Compd	Bel-7402	QSG-7701
10a	3.68 ± 0.19	>50
10d	33.87 ± 2.19	>50
10f	3.55 ± 0.17	>50
10h	4.40 ± 0.39	>50
1	0.56 ± 0.04	3.27 ± 0.25
3	3.56 ± 0.14	>50

All data are expressed as means ± SD from three separate determinations. IC_{50} values were given only if they were less than 50 μM, which was the maximum concentration tested.

of the modest potency of **10d** to Bel-7402. These findings further confirmed that the polyamine moiety may elevate the sensitivity of the conjugates toward cancer cells compared to normal cells. More importantly, these conjugates are almost nontoxic to human normal hepatocyte cells while lead compound **1** exhibited potent toxicity to both cancerous and normal cells though the cell selectivity exists to some extent. Similar results for **1** were observed in a B16 and normal Mel-A trial.[11] In this respect, naphthalimide as a cargo might be superior to anthracenes.

Evidence supports that polyamine conjugates could harness PAT to enter targeted cells.[11,12] However, prior reports didn't establish the direct relationship between PAT and cell selectivity. There are several accepted approaches for PAT evaluation, the DFMO/Spd method possesses the advantage that it is suitable to appraise most cell lines. Together with the additional experiments of tumor *versus* normal cell selectivity, the drug delivery system of polyamine conjugates *via* PAT will be evaluated more comprehensively.

Whether the naphthalimides vectored by polyamines can recognize PAT was examined by the MTT assay with DFMO (α-difluoromethylornithine) or Spd (spermidine) treated HepG2 cells (Table 3). The inhibition of the cellular polyamine biosynthesis by DFMO generally facilitates the import of exogenous polyamine *via* PAT. At the same time, polyamine conjugates will have more

Table 3 *In vitro* activity of polyamine conjugates on HepG2 cells

	IC_{50}(μM)		
Compd	—	+DFMO	+Spd
10a	11.35 ± 0.59	7.98 ± 1.18	>50
10c	2.98 ± 0.31	1.47 ± 0.25	>50
10g	15.07 ± 1.56	10.36 ± 1.42	>50
10i	8.37 ± 1.95	6.84 ± 1.36	>50

All data are expressed as means ± SD from three separate determinations. IC_{50} values were given only if they were less than 50 μM, which was the maximum concentration tested.

chances to enter the cells, and a lowering of their respective IC_{50} values in the presence of DFMO is often observed. In addition, Spd rescue experiments were conducted to test whether these drugs were using the PAT for cellular entry. Because Spd is a natural PAT substrate, it should outcompete the PAT-selective drug for cellular entry and "rescue the cell" from the cytotoxic drug. Indeed, exogenous Spd is an antagonist for drug uptake and provides a significant "import-inhibition" effect with lower amounts of drug entering the cells after incubation. This is observed as a corresponding increased IC_{50} value of the drug in the presence of Spd. Indeed, the presence of additive DFMO elevated the potency of these conjugates and the additional Spd reversed the cytotoxic effects, which implied the synthesized conjugates are PAT-selective drugs.

Due to better biological properties, **10c** was chosen for further mechanistic research. As shown in Fig. 2, **10c** displayed nice cell selectivity since it was more toxic to cancerous HepG2 cells than to normal QSG-7701 cells. Interestingly, HepG2 cells were more sensitive to additional DFMO than QSG-7701 cells, which might be interpreted by the more active PAT of cancer cells. In order to provide more proofs for the cellular entrance *via* PAT, the intrinsic fluorescence of **10c** was utilized to measure its cellular concentration, and the intracellular fluorescence was detected by a high content screening system (HCS), a new quantitative cytometric technique. As shown in Fig. 3A, the intracellular fluorescent intensity of **10c** increased in a dose- and time-dependent manner. As expected, DFMO enhanced and Spd attenuated this fluorescent intensity (Fig. 3B), which implied that DFMO fostered the cellular uptake of **10c**, and the competition of Spd for PAT restricted this cellular uptake. These results firmly supported the PAT evaluation of the DFMO/Spd method. Therefore, we can at least rationalize that this PAT-mediated

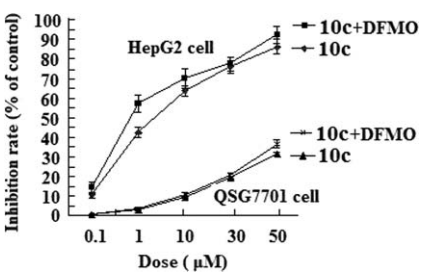

Fig. 2 Growth inhibitory effects of **10c** alone or co-treated with DFMO on HepG2 cells and QSG7701 cells. Growth inhibition was measured as described in Material and methods. Each point represents the mean ± S.D. from four independent experiments.

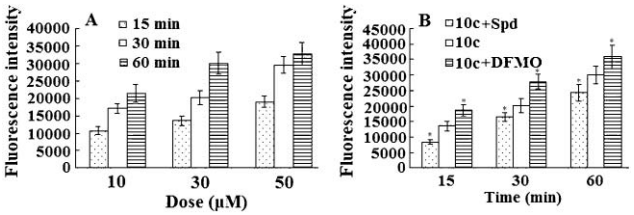

Fig. 3 The intracellular fluorescence intensity of **10c** was detected in HepG2 cells by high content screening (HCS) analysis. HepG2 cells were seeded into 96-well plates at 5×10^3 cells/well. After 24 h, the cells were stained with acridine orange (50 μg/mL) for 15 min, then washed 3 times with PBS. (A). **10c** (10, 30 or 50 μM) was added into 96-well plate and then the intracellular fluorescence intensity of **10c** for different times (15, 30, 60 min) was detected using Thermo Scientific Cellomics ArrayScan Vti. (B). **10c** (30 μM) was added into 96-well plate alone or in combination with DFMO (100 μM) and Spd (500 μM) and then the intracellular fluorescence intensity of **10c** for different times (15, 30, 60 min) was detected using Thermo Scientific Cellomics ArrayScan Vti. Each point represents the means ± S.E. from four independent experiments. Note compared with **10c**, $^*p < 0.05$.

process is beneficial for the drug to discriminate cancer cells from the normal ones which are supposed to own less active polyamine transporter.

HepG2 cell apoptosis

Apoptosis, or namely programmed cell death, can be triggered by several stimuli.[13] Both naphthalimides and polyamine derivatives could trigger cell apoptosis.[14,15] Preliminary results showed that the naphthalimide homospermidine conjugate (**3**) might produce cytotoxicity through apoptosis.[8] However, the detailed mechanism has not been delineated until now. In order to determine whether the anti-proliferative effect was associated with cell apoptosis, apoptosis was first quantified by assessing the fraction of cells with a sub-G1 DNA content using propidium iodide (PI) stain by flow cytometry. PI is a DNA-binding fluorochrome that intercalates in the double-helix. This method will result in free nuclei stained with PI for measurement of relative DNA content. Cells undergoing apoptosis will lose part of their DNA (due to the DNA fragmentation in later apoptosis). Those cells may be detected as a "sub-G1" population. As shown in Fig. 4A, **10c** potently induced HepG2 cell apoptosis and cell cycle arrest in G_0/G_1 phase. The percentages of sub-G1 cells were 1.4%, 23.8% at 0 μM and 1 μM of **10c**, respectively. In addition, these effects are enhanced by DFMO (from 23.8% to 36.9%), and attenuated by Spd (from 23.8% to 8.5%).

For a further assessment of apoptosis, we examined the exposure of phosphatidylserine (PS) on the cell surface by using PI and Annexin V-FITC double staining.[16] The assay is possible to differentiate between viable cells (Annexin V^-/PI^-), early apoptotic cells (Annexin V^+/PI^-) and late apoptotic/necrotic cells (Annexin V^+/PI^+). Flow cytometric analysis revealed that **10c** treatment led to significant increase of Annexin V-staining cells. Compared to the early (1.3%) and late (0.3%) apoptotic HepG2 cells in the control, they were elevated to 21.8% and 7.9% at 1 μM **10c**, 28.4% and 8.2% after co-incubation with DFMO. However, the additive Spd reversed the corresponding influences to 7.4% and 3.7% respectively (Fig. 4B). The results from the above two methods are in perfect agreement with each other.

We have reported that homospermidine conjugates (**1**, **3**) might induce tumor cell apoptosis *via* a mitochondrial pathway.[10] In the mitochondrial pathway, mitochondria have a crucial position in apoptosis control. The loss of mitochondria membrane potential (MMP) induces cytochrome *c* release from the mitochondria to the cytoplasm, which leads to the activation of caspase-9 and downstream cleavage of caspase-3. To explore whether a mitochondrial signal pathway was involved in **10c** induced HepG2 cell apoptosis, we examined the change of MMP and cytochrome *c* protein expression.

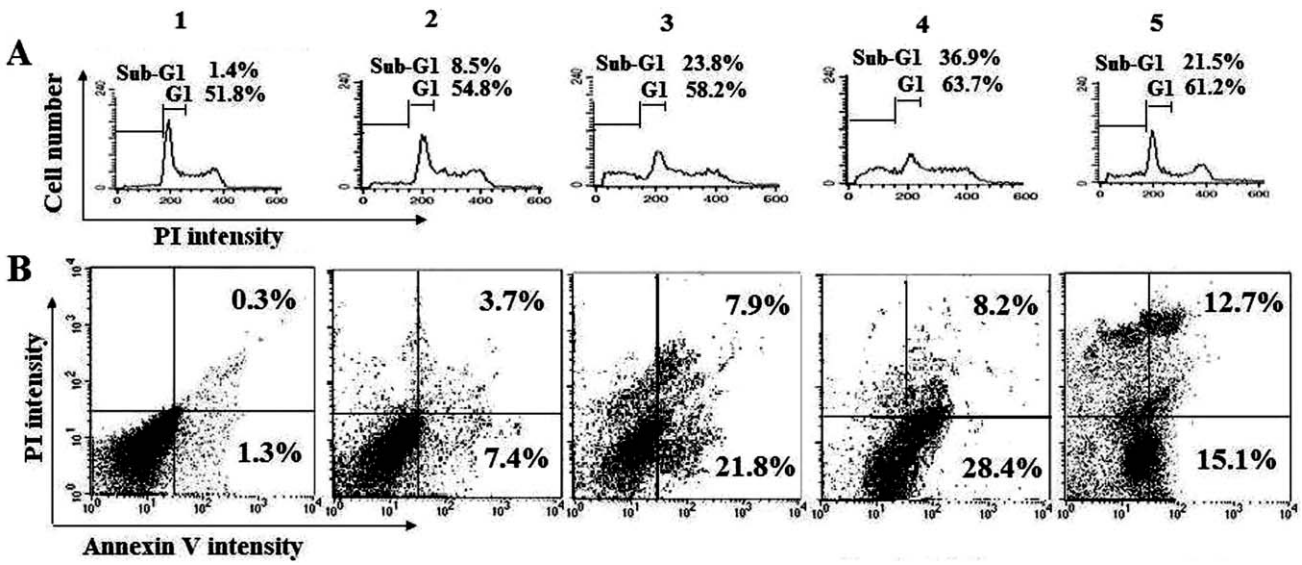

Fig. 4 **10c** alone or co-treated with DFMO or Spd induced cell apoptosis and cell cycle arrest. (A) Cell cycle was detected by PI staining. Line 1, control; Line 2, Spd+**10c**; Line 3, **10c**; Line 4, DFMO+**10c**; Line 5, rapamycin. Rapamycin (1 nM) is used as positive control. (B) Cell apoptosis was evaluated by AnnexinV–FITC apoptosis detection kit. Line 1, control; Line 2, Spd+**10c**; Line 3, **10c**; Line 4, DFMO+**10c**; Line 5, wortmannin. Wortmannin (200 nM) is used as positive control.

Rh123, a positive ion stain, can accumulate selectively in mitochondria and subsequently aggregate as a function of the membrane potential. The dysfunction of mitochondria will be accompanied by a significant decrease of fluorescence intensity due to the loss of Rh123. Indeed, great changes of MMP from 2.3% in the control to 38.5% with **10c** treatment were observed. Added Spd and DFMO with **10c** displayed contrary effects on mitochondria (Fig. 5A). As a result of MMP loss, the cytochrome *c* release from mitochondria to the cytosol with the up-regulated level of cytochrome *c* in the cytoplasm and the corresponding down-regulation of cytochrome *c* in mitochondria were observed (Fig. 5B). The followed activation of caspase-9 and downstream cleavage of caspase-3 (Fig. 5C) finally triggered HepG2 cell apoptosis.

Bcl-2 and Bcl-xL are anti-apoptotic Bcl-2 family proteins which inhibit the release of certain pro-apoptotic factors from mitochondria.[17] To understand the role of these proteins in **10c** treated HepG2 cells, the expression of Bcl-2 proteins was analyzed. Our data demonstrated that anti-apoptotic Bcl-2 family members, such as Bcl-2 and phospho-Bad (p-Bad), were markedly down-regulated, while Bcl-xL was only slightly affected (Fig. 5D).

Bad, one Bcl-xL/Bcl-2 associated death promoter homologue, is a unique Bcl-2 family member which is involved in the control of the apoptotic process in cells. 14-3-3 is a family of conserved regulatory molecules expressed in all eukaryotic cells and has the ability to bind a multitude of functionally diverse signaling proteins, including kinases, phosphatases, and transmembrane receptors.[18] In response to ligands such as IGF-1 and insulin, a variety of kinases, *e.g.* Akt and Pka, are activated and catalyze the phosphorylation of Bad on Ser-112, -136, and/or -155. These phosphorylations cooperatively mediate 14-3-3 binding, which interferes with the ability of Bad to bind and inhibit Bcl-2 or Bcl-xL. The net outcome of 14-3-3 binding to Bad is an inhibition of apoptosis and the promotion of cell survival.[19] Our research indicated that **10c** potently decreased the expression of 14-3-3, which was beneficial for the process of apoptosis.

10c inhibited the Akt phosphorylation

Though many studies reveal that polyamine derivatives induce cell apoptosis, their upstream-target in the apoptotic signaling pathway is still unclear. Akt, a protein serine/threonine kinase, is a central node in a complicated cascade of signaling pathway.[20] Therefore, we searched the Akt change after treatment **10c** in HepG2 cells using HCS, and found **10c** obviously inhibited Akt phosphorylation. As shown in Fig. 6A, the green fluorescence represents the level of Akt phosphorylation. After IGF-I treatment, the green fluorescence in control cells was significantly increased, suggesting Akt has been phosphorylated. However, the phosphorylation was notably inhibited by **10c** and almost complete dephosphorylation was observed with additional DFMO, while this effect was attenuated by Spd.

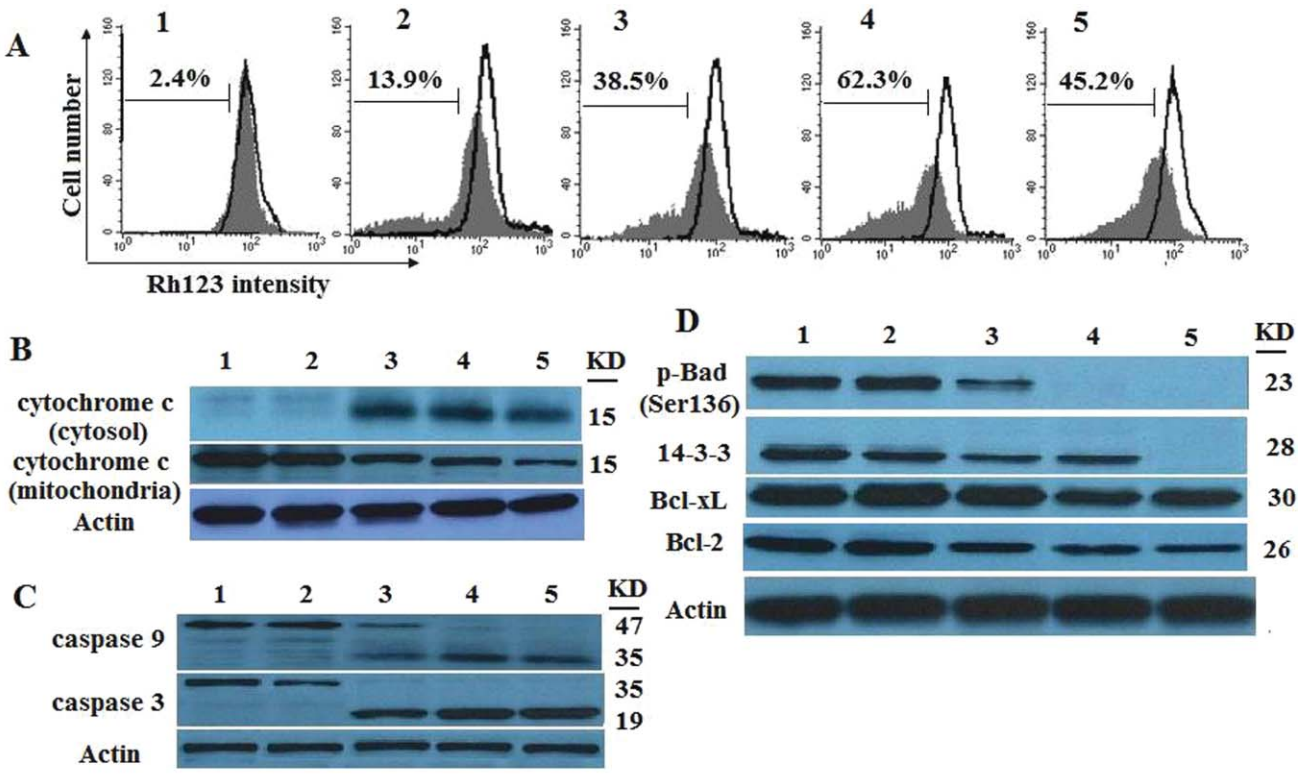

Fig. 5 **10c** alone or co-treated with DFMO or Spd triggers HepG2 cell apoptosis *via* mitochondrial pathway. (A) MMP was assessed using Rh123 by FACS. (B) Western blot analysis of the protein expression of cytochrome c. (C) Western blot analysis of the protein expression of p-Bad, Bcl-2, 14-3-3 and Bcl-xL. (D) Western blot analysis of the protein expression of caspase-9 and caspase-3. The level of each protein was determined using specific antibodies as described in Materials and Methods. β-Actin protein was blotted as a control. Line 1, control; Line 2, Spd+**10c**; Line 3, **10c**; Line 4, DFMO+**10c**; Line 5, wortmannin (200 nM). Wortmannin (200 nM) is used as positive control.

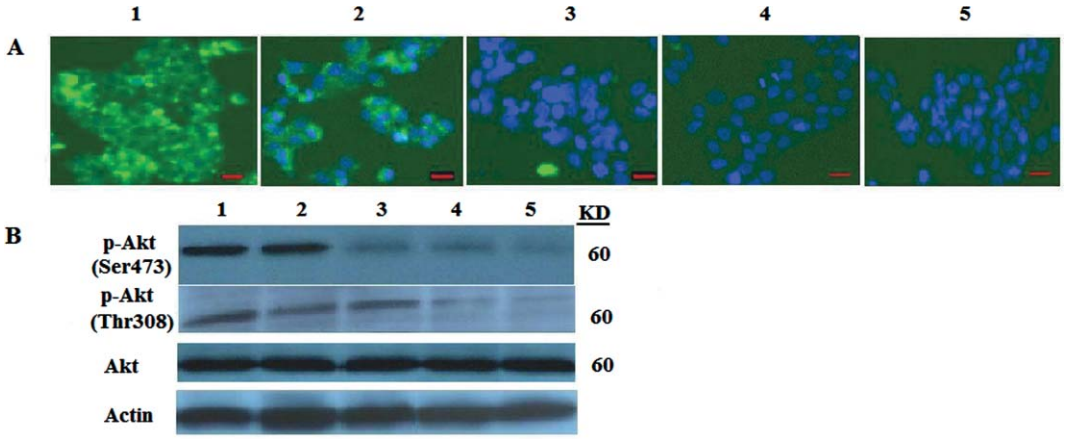

Fig. 6 **10c** alone or co-treated with DFMO or Spd inhibited Akt1 activation by HCS analysis and Western blot. (A) Akt1 translocation evaluation was performed by phospho-Akt Activation Kit in HepG2 cell. (B) Western blot analysis of the protein expression of p-Akt (Ser473 and Thr308) and Akt. The level of each protein was determined using specific antibodies as described in Materials and Methods. β-Actin protein was blotted as a control. Line 1, control; Line 2, Spd+**10c**; Line 3, **10c**; Line 4, DFMO+**10c**; Line 5, wortmannin. IGF-1 (100 nM) is used as reference agonist and wortmannin (200 nM) as reference antagonist. Bar = 50 μM.

To further confirm this effect, we detected the protein expression of Akt and phosphorylated Akt in HepG2 cells. As shown in Fig. 6B, the level of phosphorylated Akt was significantly down-regulated after cells were treated with **10c** alone or co-treated with DFMO. However, the level of total Akt protein remains constant, even in the presence of DFMO, suggesting that the observed changes of p-Akt might reflect the drop of kinase activity rather than the decrease of cellular protein content.

Cell cycle arrest

Cell cycle arrest is one of the typical responses exhibited by proliferating eukaryotic cells when exposed to a variety of cytotoxic agents.[21] As shown in Fig. 4A, **10c** induced HepG2 cell cycle arrest at G0/G1 phase, with G_0/G_1 phase cells of 51.8% at 0 μM and 58.2% at 1 μM of **10c** respectively. Exogenous Spd to **10c** provided 54.8% of G_0/G_1 phase cells, and added DFMO increased the percentage of G_0/G_1 cells to 63.7%.

We then examined the expression of the cyclin-dependent kinase 4 (Cdk4) and its inhibitor, $p27^{Kip1}$, which play a critical role in the entry of quiescent G0 phase cells into the cell cycle. Being present at maximal levels in quiescent cells, the decreased amount of $p27^{Kip1}$ will stimulate cells to enter the cell cycle, thereby allowing the activation of G1 phase Cdk/cyclin complexes with subsequent cell cycle progression.[22] In comparison to the control, **10c** increased the level of $p27^{kip1}$, especially in the presence of DFMO. Accordingly, the expression of Cdk4 was significantly down-regulated, and DFMO exerted a potent synergistic effect (Fig. 7). These results are consistent with the role of these proteins in the regulation of the G1 phase transition.

Akt/mTOR signal pathway is often involved with cell cycle progress. The mammalian target of rapamycin (mTOR) is a key downstream kinase of Akt, which regulates tumor cell proliferation, growth, survival and angiogenesis.[23] Akt/mTOR generally acts to promote survival through inhibition of proapoptotic factors and activation of anti-apoptotic factors.[24] The 70 kDa ribosomal S6 kinase (p70S6K) is a downstream-target of mTOR and regulates protein synthesis, proliferation, and cell cycle

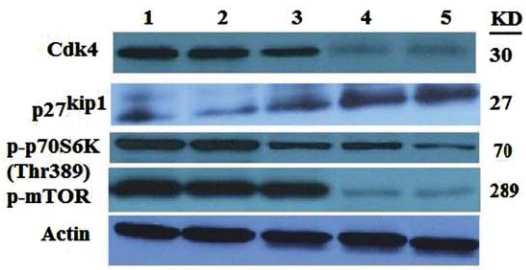

Fig. 7 The protein expression of Cdk4 and $p27^{kip1}$, p-p70S6K and p-mTOR analysed by Western blot. The level of each protein was determined using specific antibodies as described in Materials and Methods. β-Actin protein was blotted as a control. Line 1, control; Line 2, Spd+**10c**; Line 3, **10c**; Line 4, DFMO+**10c**; Line 5, rapamycin. Rapamycin (1 nM) is used as a positive control.

control. The role of ribosomal p70S6K in the cell cycle has been studied extensively, and it is known that this enzyme is crucial for cell advancement through G1.[20] Only after being phosphorylated, the function of mTOR and p70S6K is activated. So we detected the expression of p-mTOR and p-p70S6K in the presence of **10c**. The expression of p-mTOR was slightly down-regulated, however, co-treatment with DFMO greatly strengthened the effect of **10c**. In contrast, **10c** negatively regulated p-p70S6K expression evidently, but this effect was obviously attenuated by extra Spd (Fig. 7). These results indicated that **10c** regulated cell cycle *via* the Akt/mTOR pathway.

Conclusion

Extensive studies suggest that polyamines are promising vehicles for cytotoxic agents that might otherwise be poorly transported into tumour cells.[5] Indeed, when proper goods such as naphthalimides were attached to polyamine motifs, the resulting conjugates could be effectively transported into cells *via* PAT, and thus displayed excellent tumor selectivity. Importantly, elevated potency with DFMO provided a basis for possible co-administration therapies.

Compound **10c** could suppress the Akt phosphorylation at Ser473 and Thr308 and its kinase activity, suggesting it is an inhibitor of the Akt signaling pathway, but not directly of Akt. Inhibiting Akt phosphorylation triggered a series of downstream cellular functions, including MMP decrease, cytochrome *c* release from mitochondria to cytoplasm, down-regulation of the anti-apoptotic protein expression such as p-Bad and Bcl-2, and finally induced mitochondrial apoptosis. Preliminary data also demonstrated that **10c** could inhibit HepG2 cell growth by cell cycle arrest at G0/G1 phase. The down-regulated expression of p70SK, p-mTOR and Cdk4 and the elevated expression of $p27^{kip1}$ proved that the Akt/mTOR signaling pathway is correlated with the cell cycle progress triggered by **10c**.

In recent years, a number of cancer researchers have focused on the central importance of the Akt/mTOR pathway which is often over-expressed in many tumor cells, and diverse Akt/mTOR pathway inhibitors are now being developed.[25] To our knowledge, this is the first report to provide proof of the mechanistic basis of apoptosis and cell cycle arrest induced by naphthalimide polyamine conjugates *via* the Akt/mTOR signal pathway. Detailed experiments strongly suggested that **10c** targeted both PAT on membrane for drug delivery and cellular Akt/mTOR signaling pathway for antitumor effects. Therefore, **10c** could be a promising candidate for the development of novel class of polyamine-based Akt/mTOR pathway inhibitors.

Experimental protocols

Synthesis of naphthalimide polyamine conjugates

All chemicals (reagent grade) used were commercially available. Melting points were determined on a X-6 hot stage microscope and were uncorrected. All the ^{1}H NMR and ^{13}C NMR spectra were recorded on a Bruker AV-400 model Spectrometer in D_2O. Chemical shifts for ^{1}H NMR and ^{13}C NMR spectra were reported in parts per million to residual solvent protons. ESI-MS spectra were recorded on an ESQUIRE-LC Mass spectrometer. Elemental analyses were performed on a Gmbe VarioEL Elemental Instrument.

General procedure for the preparation of 10a–10i

The Boc protected tetraamine (**8a**–**8c**, 1.1 mmol) was dissolved in anhydrous ethanol (30 mL). After the mixture was stirred for 15 minutes at ambient temperature, a naphthalic anhydride (**4**–**7**, 1mmol) was added, then the reaction mixture was refluxed for 4 h. The volatiles were removed under vacuum to give a residue. The residue was subjected to flash chromatography (25% Petroleum/EtOAc, v/v) to obtain intermediates **9a**–**9i**.

Pure **9** was immediately dissolved in EtOH (20 mL) and stirred at 0 °C for 10 min. 4M HCl (15 mL) was added dropwise at 0 °C. The reaction mixture was stirred at room-temperature overnight. The solution typically gave a bright white or yellow solid as a precipitate. The solid was filtered, washed several times with absolute ethanol and dried under vacuum to give the pure target compounds (**10a**–**10i**).

2-{3-[3-(3-Aminopropylamino)propylamino]propyl}-1*H*-6-chlorobenz-[*de*]isoquinoline-1,3(2*H*)-dione trihydrochloride (10a) yield 55.7%; m.p.: 279–281 °C; ^{1}H NMR (D_2O, 400 MHz) δ: 7.73 (d, 1H, $J = 7.2$ Hz), 7.69 (d, 1H, $J = 8.0$ Hz), 7.48 (d, 1H, $J = 7.6$ Hz), 7.26 (t, 1H, $J = 7.6$ Hz), 7.17 (d, 1H, $J = 8.0$ Hz), 3.82 (t, 2H, $J = 7.2$ Hz), 3.10–3.27 (m, 10H), 2.10–2.24 (m, 4H), 1.93–2.00 (m, 2H); ^{13}C NMR (D_2O) δ: 163.61, 163.24, 139.11, 131.82, 130.82 (2C), 127.75, 127.12, 127.06 126.20, 119.73, 118.30, 45.50, 44.77, 44.69 (2C), 37.52, 36.58, 24.19, 23.78, 22.75; ESI-MS *m/z*: 403.3 $(M+H-3HCl)^+$; Anal. calcd. for $C_{21}H_{30}Cl_4N_4O_2 \cdot 1.3H_2O$: C, 47.08; H, 6.13; N, 10.46; found: C, 46.96; H, 6.09; N, 10.30.

2-{3-[4-(3-Aminopropylamino)butylamino]propyl}-1*H*-6-chlorobenz-[*de*]isoquinoline-1,3(2*H*)-dione trihydrochloride (10b) yield: 66.4%; m.p.: 276.5–278 °C; ^{1}H NMR (D_2O, 400 MHz) δ: 7.80 (d, 1H, $J = 7.2$ Hz), 7.75 (d, 1H, $J = 8.0$ Hz), 7.55 (d, 1H, $J = 7.6$ Hz), 7.32 (t, 1H, $J = 7.6$ Hz), 7.24 (d, 1H, $J = 7.6$ Hz), 3.86 (t, 2H, $J = 7.2$ Hz), 3.15–3.25 (m, 10H), 2.12–2.20 (m, 2H), 2.00–2.04 (m, 2H), 1.82–1.88 (m, 4H); ^{13}C NMR (D_2O) δ: 163.73, 163.37, 139.16, 131.89, 130.86 (2C), 127.82 (2C), 127.18, 126.34, 119.88, 118.45, 47.11 (2C), 45.35, 44.64, 37.59, 36.66, 24.24, 23.81, 22.89 (2C); ESI-MS *m/z*: 417.3 $(M+H-3HCl)^+$; Anal. calcd. for $C_{22}H_{32}Cl_4N_4O_2 \cdot 1.0H_2O$: C, 48.54; H, 6.30; N, 10.29; found: C, 48.34; H, 6.32; N, 10.60.

2-{4-[4-(4-Aminobutylamino)butylamino]butyl}-1*H*-6-chlorobenbenz-[*de*]isoquinoline-1,3(2*H*)-dione Trihydrochloride (10c) yield: 46%; m.p.: 287.0–288.5 °C; ^{1}H NMR (D_2O, 400 MHz) δ: 7.62 (d, 2H, $J = 8.0$ Hz), 7.38 (d, 1H, $J = 8.0$ Hz), 7.19 (t, 1H, $J = 7.6$ Hz), 7.11 (d, 1H, $J = 7.6$ Hz), 3.63 (t, 2H, $J = 6.8$ Hz), 2.98–3.09 (m, 10H), 1.55–1.78 (m, 12H); ^{13}C NMR (D_2O) δ: 163.50, 163.14, 138.95, 131.65, 130.66 (2C), 127.63, 127.03, 126.96, 126.06 119.72, 118.30, 47.12, 46.93, 46.90 (2C), 39.77, 38.79, 24.13, 23.92, 23.24, 22.87, 22.84, 22.77; ESI-MS *m/z*: 445.2 $(M+H-3HCl)^+$; Anal. calcd. for $C_{24}H_{36}Cl_4N_4O_2 \cdot 1.0H_2O$: C, 50.36; H, 6.69; N, 9.79; found: C, 50.71; H, 6.75; N, 10.00.

2-{3-[4-(3-Aminopropylamino)butylamino]propyl}-1*H*-6-bromobenz-[*de*]isoquinoline-1,3(2*H*)-dione trihydrochloride (10d) yield: 64.8%; m.p.: 287.5–289.5 °C; ^{1}H NMR (D_2O, 400 MHz) δ: 7.74 (d, 1H, $J = 7.2$ Hz), 7.63 (d, 1H, $J = 8.4$ Hz), 7.35–7.40 (m, 2H), 7.25 (t, 1H, $J = 8.0$ Hz), 3.82 (t, 2H, $J = 6.4$ Hz), 3.03–3.20 (m, 10H), 2.07–2.15 (m, 2H), 1.95–1.99 (m, 2H), 1.76–1.83 (m, 4H); ^{13}C NMR (D_2O) δ: 163.56, 163.43, 133.33, 132.33, 132.88, 131.41, 130.75, 128.38, 127.94, 126.04, 119.80, 118.90, 47.07 (2C), 45.31, 44.59, 37.61, 36.58, 24.18, 23.77, 22.85 (2C); ESI-MS *m/z*: 463.0 $(M+H-3HCl)^+$; Anal. calcd. for $C_{22}H_{32}BrCl_3N_4O_2 \cdot 1.0H_2O$: C, 44.88; H, 5.82; N, 9.52; found: C, 44.53; H, 5.85; N, 9.85.

2-{3-[4-(3-Aminopropylamino)butylamino]propyl}-1*H*-5-nitrobenz-[*de*]isoquinoline-1,3(2*H*)-dione trihydrochloride (10e) yield: 70.2%; m.p.: 216.5–217.5 °C; ^{1}H NMR (D_2O, 400 Hz) δ: 8.77 (d, 1H, $J = 2.0$ Hz), 8.45 (d, 1H, $J = 2.4$ Hz), 8.35 (d, 1H, $J = 8.8$ Hz), 8.18 (d, 1H, $J = 7.6$ Hz), 7.76 (t, 1H, $J = 7.6$ Hz), 4.05 (t, 2H, $J = 6.4$ Hz), 3.05–3.23 (m, 10H), 2.10–2.18 (m, 4H), 1.79–1.87 (m, 4H); ^{13}C NMR (D_2O) δ: 163.87, 163.06, 145.04, 136.78, 134.91, 130.09, 130.00, 129.52, 128.52, 123.18, 122.29, 120.87, 47.09, 47.03, 45.32, 44.61, 37.71, 36.62, 24.24, 23.80, 22.86 (2C); ESI-MS *m/z*: 428.3 $(M+H-3HCl)^+$; Anal. calcd. for $C_{22}H_{32}Cl_3N_5O_4 \cdot 1.3H_2O$: C 47.16; H, 6.22; N, 12.50 found: C 47.08; H, 6.23; N, 12.68.

2-{4-[4-(4-Aminobutylamino)butylamino]butyl}-1*H*-5-nitrobenz-[*de*]isoquinoline-1,3(2*H*)-dione trihydrochloride (10f) yield: 66.8%; m.p.: 235.5–237.0 °C; ^{1}H NMR (D_2O, 400 MHz) δ: 8.70 (s, 1H), 8.34 (s, 1H), 8.22 (1H, d, $J = 7.2$ Hz), 8.09 (1H, d, $J = 8.0$ Hz), 7.67 (t, 1H, $J = 7.6$ Hz), 3.85 (t, 2H, $J = 6.8$ Hz),

3.03–3.12 (m, 10H), 1.67–1.79 (m, 12H); ^{13}C NMR (D_2O) δ: 163.12, 162.77, 144.91, 136.56, 134.66, 129.93, 129.76, 129.37, 128.31, 122.94, 122.21, 120.80, 47.15, 46.92, 46.89, 46.87, 39.88, 38.80, 24.17, 23.92, 23.18, 22.84 (2C), 22.76; ESI-MS *m/z*: 456.3 $(M+H-3HCl)^+$; Anal. calcd. for $C_{24}H_{36}Cl_3N_5O_4 \cdot 1.1H_2O$: C, 49.30; H, 6.58; N, 11.98; found: C, 49.57; H, 6.49; N, 11.60.

5-Amino-2-{3-[3-(3-aminopropylamino)propylamino]propyl}1*H*-benz-[*de*]isoquinoline-1,3-(2*H*)-dione tetrahydrochloride (10g) yield: 68.3%; m.p.: 270–272 °C; ^{1}H NMR (D_2O, 400 MHz) δ: 7.92 (d, 1H, J = 1.6 Hz), 7.90 (d, 1H, J = 2.8 Hz), 7.87 (d, 1H, J = 2.4 Hz), 7.80 (d, 1H, J = 2.0 Hz), 7.48 (t, 1H, J = 7.6 Hz), 3.93 (t, 2H, J = 7.2 Hz), 3.11–3.24 (m, 10H), 2.04–2.21 (m, 4H), 1.99–2.04 (m, 2H); ^{13}C NMR (D_2O) δ: 164.37, 163.85, 134.33, 132.70, 131.25 131.09, 128.15, 125.41, 124.61, 124.32, 122.17, 120.15, 45.55, 44.75, 44.67, 44.62, 37.45, 36.58, 24.24, 23.76, 22.72; ESI-MS *m/z*: 384.3 $(M+H-4HCl)^+$; Anal. calcd. for $C_{21}H_{33}Cl_4N_5O_2 \cdot 2.22H_2O$: C, 44.33; H, 6.63; N, 12.31; found: C, 44.70; H, 6.97; N, 11.96.

5-Amino-2-{3-[4-(3-aminopropylamino)butylamino]propyl}1*H*-benz-[*de*]isoquinoline-1,3(2*H*)-dione tetrahydrochloride (10h) yield: 62.9%; m.p.: 262.5–264.0 °C; ^{1}H NMR (D_2O, 400 MHz) δ: 7.85 (s, 1H), 7.83 (d, 1H, J = 1.6 Hz), 7.78 (d, 1H, J = 2.0 Hz), 7.70 (d, 1H, J = 2.0 Hz), 7.42 (t, 1H, J = 7.6 Hz), 3.89 (t, 2H, J = 7.2 Hz), 3.11–3.21 (m, 10H), 2.08–2.16 (m, 2H), 1.96–2.04 (m, 2H), 1.82–1.83 (m, 4H); ^{13}C NMR (D_2O) δ: 164.29, 163.78, 134.19, 133.43, 131.22, 130.79, 128.03, 124.74, 124.23, 124.10, 121.95, 120.00, 47.07 (2C), 45.37, 44.60, 37.48, 36.63, 24.25, 23.78, 22.85 (2C); ESI-MS *m/z*: 398.3 $(M+H-4HCl)^+$; Anal. calcd. for $C_{22}H_{35}Cl_4N_5O_2 \cdot 1.6H_2O$: C, 46.18; H, 6.73; N, 12.24; found: C, 46.25; H, 7.07; N, 11.96.

5-Amino-2-{4-[4-(4-aminobutylamino)butylamino]butyl}1*H*-benz-[*de*]isoquinoline-1,3(2*H*)-dione tetrahydrochloride (10i) yield: 61.9%; m.p.: 262–264 °C; ^{1}H NMR (D_2O, 400 MHz) δ: 7.75–7.80 (m, 3H), 7.68 (s, 1H), 7.37 (t, 1H, J = 8.0 Hz), 3.75 (t, 2H, J = 6.8 Hz), 3.03–3.12 (m, 10H), 1.61–1.80 (m, 12H); ^{13}C NMR (D_2O) δ: 164.12, 163.64, 134.05, 132.87, 131.10, 130.80, 128.02, 124.98, 124.28, 124.10, 122.07, 120.04, 47.23, 46.96, 46.92 (2C), 39.78, 38.86, 24.20, 23.96, 23.24, 22.87, 22.86, 22.78; ESI-MS *m/z*: 426.4 $(M+H-4HCl)^+$; Anal. calcd. for $C_{24}H_{39}Cl_4N_5O_2 \cdot 4.6H_2O$: C, 44.06; H, 7.43; N, 10.70; found: C, 44.05; H, 7.42; N, 10.59.

Biological materials and methods

Material

RNase A, rhodamine123 (Rh123), 3-(4,5-dimethylthiazol)-2,5-diphenyltetrazolium bromide (MTT), rapamycin, wortmannin and propidium iodide (PI) were purchased from Sigma (St. Louis, MO, USA). RPMI1640, F12 and Fetal calf serum (FCS) were purchased from Gibco (Grand Island, NY, USA). AnnexinV–FITC apoptosis detection kit was purchased from Cell Signaling Technology (Beverly, MA, USA). Proteins were detected by Western blotting using the following primary antibodies: Akt, phospho-Akt(Thr308), phospho-Akt(Ser473), phospho-p70S6 kinase (Thr389), phospho-mTOR were purchased from Cell Signaling Technology (Beverly, MA, USA); Bcl-xL, phospho-Bad (Ser136), 14-3-3, caspase-9, caspase-3, Cdk4, $p27^{kip1}$, Bcl-2 and cytochrome *c*, as well as horseradish peroxidase-conjugated anti-mouse and anti-rabbit antibodies were purchased from Santa Cruz Biotechnologies (Santa Cruz, CA, USA). All other chemicals used in the experiments were commercial products of reagent grade. Stock solution (10 mM) was prepared in DMSO and diluted to various concentrations with serum-free culture medium.

Cell culture and treatments

HepG2 cell line and QSG-7701 cell line were purchased from Shanghai Institutes for Biological Science, Chinese Academy of Sciences (Shanghai, China). K562, MDA-MB-231, LnCap and Bel-7402 cell lines were obtained from American Type Culture Collection (ATCC, USA). Cells were cultured in RPMI1640, supplemented with 10% heat-inactivated fetal calf serum (FCS) or 20% heat-inactivated FCS for QSG-7701 cells and antibiotics (penicillin, 100 units/mL; streptomycin sulfate, 100 μg/mL) at 37 °C, in an atmosphere of 95% air and 5% CO_2 under humidified conditions. Aminoguanidine (1 mM) was added as an inhibitor of amine oxidase derived from FCS and had no effect on the various parameters of the cell measured in this study.[10] For the *in vitro* activation of Akt and mTOR kinases, cells were seeded overnight and then serum starvation for 24 h, followed by treatment with IGF-1 (100 ng/mL, Calbiochem, USA) for 10 min.

MTT assay

Chemosensitivity was assessed using the 3-(4,5-dimethylthiazol-2-yl)-2,5-diphenyltetrazolium bromide (MTT) assay. Briefly, exponentially growing K562 cells were seeded into 96-well plates at 4000 cells/well and treated with indicated concentrations of samples for 48 h, and then 10 μL of MTT (10 mg/mL) was added. After incubation for 4 h at 37 °C, the purple formazan crystals (*i.e.* a reduced form of MTT) generated from viable cells were dissolved by adding 100 μL 10% sodium dodecyl sulfate (SDS) in each well. The absorbance of each well was then read at 570 nm.

In addition, exponentially growing MDA-MB-231, LnCap, Bel-7402 and QSG-7701 cells were seeded into 96-well plates at 5000 cells/well and allowed to attach overnight. The above cells were treated with the indicated concentration of samples for 48 h, and then 100 μL of MTT (1 mg/mL) was added. After incubation for 4 h at 37 °C, the MTT solution was removed and the remaining formazan crystals were dissolved with 150 μL DMSO in each well. The absorbance of each well was then read at 570 nm.

The cytotoxicity of **10c**, in the presence or absence of 100 μM DFMO or 500 μM Spd, was evaluated in HepG2 cells and QSG-7701 cells by the conversion of MTT to a purple formazan precipitate as previously described.[26] The concentration of DFMO (100 μM) and Spd (500 μM) is selected for no obvious cytotoxicity on HepG2 cells and QSG-7701 cells and the inhibition ratio is 2.76%, 0.34% and 0.74%, 0.18%, respectively. Cells were seeded into 96-well plates at 5×10^3 cells/well. Various concentrations of **10c** with or without 100 μM DFMO or 500 μM Spd were subsequently added and incubated for 48 h. The inhibited rate was calculated from plotted results using untreated cells as 100%.

Intracellular fluorescence intensity assay

The intracellular fluorescent intensity of **10c** was detected in HepG2 cells by high content screening (HCS) (Thermo Scientific Cellomics ArrayScan Vti, Cellomics, Inc., Pittsburgh, USA) analysis which is a new quantitative cytometric technique. Briefly, HepG2 cells were seeding into 96-well plates at 5×10^3 cells/well.

After 24 h, the cells were stained with acridine orange (50 μg/mL) for 15 min, then washed 3 times with PBS. **10c** (10, 30 or 50 μM) was added into a 96-well plate alone or combination with DFMO (100 μM) and Spd (500 μM) and then the intracellular fluorescent intensity of **10c** for different times (15, 30, 60 min) was detected using Thermo Scientific Cellomics ArrayScan Vti. Cell numbers was determined using AO staining and intracellular fluorescent intensity of **10c** was then detected at excitation wavelength of 350 nm and emission wavelength of 460 nm.

Cell apoptosis evaluation

Cell apoptosis was evaluated by two methods. Firstly, after exposed to **10c** (1 μM) in the presence or absence of 100 μM DFMO or 500 μM Spd for 48 h, cells were fixed with ice-cold 70% ethanol and then stained with PI (100 μg/mL) after removing the RNA in the cells by RNase A treatment (50 μg/mL). Data acquisition and analysis were controlled by Modifit software. Secondly, apoptotic evaluation was performed by AnnexinV-FITC apoptosis detection kit. Cells were seeded in six-well plates, and exposed to **10c** in the absence or presence of 100 μM DFMO or 500 μM Spd for 48 h, then harvested and stained according to manufacturer's instruction. Data acquisition and analysis were controlled by cellquest software.[27] Rapamycin (1 nM), a specific mTOR inhibitor, was used as positive control.

Akt activation analysis by HCS assay

A new quantitative cytometric technique analysis (HCS) was used to measure Akt activity on HepG2 cells by Thermo Scientific Cellomics ArrayScan Vti (KSR, Cellomics, Inc., Pittsburgh, PA). For HepG2 cells, Akt1 translocation evaluation was performed by phospho-Akt Activation Kit (Cellomics, No. 8404102). Cells were seeded in 96-well plates, and exposed to **10c** in the absence or presence of 100 μM DFMO or 500 μM Spd for 48 h, then stained according to the manufacturer's instruction and read on a Thermo Scientific Cellomics ArrayScan Vti and Morphology Explorer BioApplication Software Module. Insulin-like growth factor-I (IGF-I) was used as reference agonist, and compounds were assayed for their ability to inhibit IGF-I-stimulated membrane translocation of Akt1. The PI3K inhibitor wortmannin (200 nM) was used as reference antagonist.

Measurement of MMP

MMP was assessed by the retention of Rh123, a membrane-permeable fluorescent cationic dye. The uptake of Rh123 by mitochondria is proportional to the MMP.[26] Briefly, cells (1×10^6) were incubated with 0.1 μg/mL Rh123 in the dark for 20 min at room temperature. After washing with PBS, the cells were analyzed by FACScan with excitation and emission wavelength of 495 and 535 nm, respectively.

Western blots

HepG2 cells, treated with **10c** and/or DFMO and Spd for 48 h, were harvested and washed with PBS. Cytosolic and mitochondrial fractions were prepared as our previous described.[25] Total cellular protein was isolated using the protein extraction buffer (containing 150 mM NaCl, 10 mM Tris (pH 7.2), 5 mM EDTA, 0.1% Triton-100, 5% glycerol and 2% SDS). Protein concentrations were determined using the protein assay kit. Equal amounts of proteins (50 μg/lane) were fractionated using 8% or 12% SDS-PAGE and transferred to PVDF membranes. The membranes were incubated with primary antibodies. After being washed with PBS, the membranes were incubated with peroxidase-conjugated goat antimouse or antirabbit secondary antibody, followed by enhanced chemiluminescence staining through the enhanced chemiluminescence system. Actin was used to normalize for protein loading.[27]

Data analysis

All data were presented as mean ± S.D. and analyzed using Students *t* test or analysis of variance (ANOVA) followed by *q* test.

Acknowledgements

This project was supported by National Natural Science Foundation of China (No. 20872027), Henan Natural Science Foundation (No. 0821022700), and China Postdoctoral Science Foundation Funded Project (No. 20090450092).

References

1 M. F. Braña and A. Ramos, *Curr. Med. Chem.: Anti-Cancer Agents*, 2001, **1**, 237–255.
2 (*a*) E. V. Quaquebeke, T. Mahieu, P. Dumont, J. Dewelle, F. Ribaucour, G. Simon, S. Sauvage, J.-F. Gaussin, J. Tuti, M. Yazidi, F. V. Vynckt, T. Mijatovic, F. Lefranc, F. Darro and R. Kiss, *J. Med. Chem.*, 2007, **50**, 4122–4134; (*b*) M. F. Braña, M. Cacho, M. A. Garcia, B. de Pascual-Teresa, A. Ramos, M. T. Dominguez, J. M. Pozuelo, C. Abradelo, M. F. Rey-Stolle, M. Yuste, M. Banez-Coronel and J. C. Lacal, *J. Med. Chem.*, 2004, **47**, 1391–1399.
3 (*a*) T. Mijatovic, T. Mahieu, C. Bruyère, N. De Nève, J. Dewelle, G. Simon, M. J. Dehoux, E. von der Aar, B. Haibe-Kains, G. Bontempi, C. Decaestecker, E. Van Quaquebeke, F. Darro and R. Kiss, *Neoplasia*, 2008, **10**, 573–586; (*b*) H. Zhu, M. Huang, F. Yang, Y. Chen, Z. H. Miao, X. H. Qian, Y. F. Xu, Y. X. Qin, H. B. Luo, X. Shen, M. Y. Geng, Y. J. Cai and J. Ding, *Mol. Cancer Ther.*, 2007, **6**, 484–495.
4 C. Wang, J.-G. Delcros, L. Cannon, F. Konate, H. Carias, J. Biggerstaff, R. A. Gardner and O. Phanstiel, *J. Med. Chem.*, 2003, **46**, 5129–5138.
5 R. A. Casero and L. J. Marton, *Nature Reviews Drug Discovery*, 2007, **6**, 373–390.
6 J. M. Barret, A. Kruczynski, S. Vispé, J. P. Annereau, V. Brel, Y. Guminski, J. G. Delcros, A. Lansiaux, N. Guilbaud, T. Imbert and C. Bailly, *Cancer Res.*, 2008, **68**, 9845–9853.
7 (*a*) C. Wang, J.-G. Delcros, J. Biggerstaff and O. Phanstiel, *J. Med. Chem.*, 2003, **46**, 2672–2682; (*b*) C. Wang, J.-G. Delcros, J. Biggerstaff and O. Phanstiel, *J. Med. Chem.*, 2003, **46**, 2663–2671; (*c*) M. L. Bolognesi, N. Calonghi, C. Mangano, L. Asotti and C. Elchiorre, *J. Med. Chem.*, 2008, **51**, 5463–5467; (*d*) C. Tsen, M. Iltis, N. Kaur, C. Bayer, J.-G. Delcros, L. Kalm and O. Phanstiel, *J. Med. Chem.*, 2008, **51**, 324–330.
8 Z. Tian, S. Xie, Y. Du, Y. Ma, J. Zhao, W. Gao and C. Wang, *Eur. J. Med. Chem.*, 2009, **44**, 393–399.
9 Q. Yang, X. Qian, J. Xu, Y. Sun and Y. Li, *Bioorg. Med. Chem.*, 2005, **13**, 1615–1622.
10 S. Xie, P. Cheng, G. Liu, Y. Ma, J. Zhao, M. Chehtane, A. R. Khaled, O. Phanstiel and C. Wang, *Bioorg. Med. Chem. Lett.*, 2007, **17**, 4471–4475.
11 R. A. Gardner, J.-G. Delcros, F. Konate, F. Breitbeil, B. Martin, M. Sigman, M. Huang and O. Phanstiel, *J. Med. Chem.*, 2004, **47**, 6055–6069.
12 N. Kaur, J.-G. Delcros, J. Imran, A. Khaled, M. Chehtane, N. Tschammer, B. Martin and O. Phanstiel, *J. Med. Chem.*, 2008, **51**, 1393–1401.

13 C. Hegardt, G. Andersson and S. M. Oredsson, *Exp. Cell Res.*, 2001, **266**, 333–341.
14 L. D. Ralton, C. S. Bestwick, L. Milne, S. Duthie, P. Kong and Thoo Lin, *Chem.-Biol. Interact.*, 2009, **177**, 1–6.
15 R. G. Schipper, L. C. Penning and A. A. Verhofstad, *Semin. Cancer Biol.*, 2000, **10**, 55–68.
16 M. van Engeland, L. J. Nieland, F. C. Ramaekers, B. Schutte and C. P. Reutelingsperger, *Cytometry*, 1998, **31**, 1–9.
17 L. Yang, D. Wu, K. Luo, S. Wu and P. Wu, *Cancer Lett.*, 2009, **276**, 180–188.
18 Y. O Al-Bazz, J. C Underwood, B. L Brown and P. R Dobson, *Eur. J. Cancer*, 2009, **45**, 694–704.
19 G. Tzivion and J. Avruch, *J. Biol. Chem.*, 2002, **277**, 3061–3064.
20 T. A Yap, M. D Garrett, M. I Walton, F Raynaud, J. S. de Bono and P. Workman, *Curr. Opin. Pharmacol.*, 2008, **8**, 393–412.
21 L. Ding, B. Liu, L. L. Qi, Q. Y. Zhou, Q. Hou, J. Li and Q. Zhang, *Toxicol. in Vitro*, 2009, **23**, 408–417.
22 D. Baiz, G. Pozzato, B. Dapas, R. Farra, B. Scaggiante, M. Grassi, L. Uxa, C. Giansante, C. Zennaro, G. Guarnieri and G. Grassi, *Biochimie*, 2009, **91**, 373–382.
23 A. Vazquez-Martin, C. Oliveras-Ferraros, L. Bernadó, E. López-Bonet and J. A. Menendez, *Biochem. Biophys. Res. Commun.*, 2009, **380**, 638–643.
24 S. S. Grewal, *Int. J. Biochem. Cell Biol.*, 2009, **41**, 1006–1010.
25 M. Hanada and J. Feng, *Biochim. Biophys. Acta.*, 2004, **1697**, 3–16.
26 S. Xie, G. Liu, Y. Ma, P. Cheng, Y. Wu, M. Wang, B. Ji, J. Zhao and C. Wang, *Toxicol. in Vitro*, 2008, **22**, 352–358.
27 B. K. Lundholt, V. Linde, F. Loechel, H. C. Pedersen, S. Møller, M. Praestegaard, I. Mikkelsen, K. Scudder, S. P. Bjørn, M. Heide, P. O. Arkhammar, R. Terry and S. J. Nielsen, *J. Biomol. Screening*, 2005, **10**, 20–29.

